Chapter 3

Biochemical Kinetics

> ...I began to lose interest in some of the things [in mathematics] that to me seemed rather remote from reality and hankered after something more practical. I realize now that I was much better fitted to engineering than to mathematics, but physiology proved in the end to be much like engineering, being based on the same ideas of function and design.
>
> –*A. V. Hill*, in *The Third Bayliss-Starling Memorial Lecture*

The study of the rates of chemical reactions is called *chemical kinetics*. In the previous chapter, we used the law of mass action to establish chemical reaction rates. In this chapter we will develop rate laws that are applicable to biochemical processes.

Individual chemical reaction events (binding, unbinding, and conversion) are called *elementary reactions*. As in the previous chapter, we will continue to use mass action to describe the rates of elementary reactions. In contrast, individual *biochemical reactions* involve small networks of elementary reactions. To develop rate laws for biochemical reactions, we will collapse these networks into single reaction events, using separation of time-scale methods. The rate laws that described these 'lumped' reaction events are referred to as *biochemical kinetics*.

3.1 Enzyme Kinetics

The overwhelming majority of reactions that occur within a cell are catalysed by **enzymes** (which are proteins). Enzymes catalyse reactions by binding the reactants (called the enzyme *substrates*) and facilitating their conversion to the reaction products. Enzyme catalysis reduces the energy barrier associated with the reaction event (Figure 3.1A). Consequently, while enzyme catalysis increases the rate at which equilibrium is attained, it has no effect on the equilibrium itself (Figure 3.1B).

The standard 'lock-and-key' model of enzyme activity is illustrated in Figure 3.2A. As shown for this reversible reaction, the enzyme catalyses the reaction in both directions and is unaltered by the reaction event. The part of the enzyme that binds the substrate is called the *active* (or *catalytic*) *site*. The active site has a shape and chemical structure that is complementary to the substrate, resulting in strong binding affinity and a highly specific interaction. Enzymes typically bind only a single substrate species, and most catalyse only a specific reaction. This specificity of action allows each enzyme to function with remarkable efficiency—increasing reaction rates by as

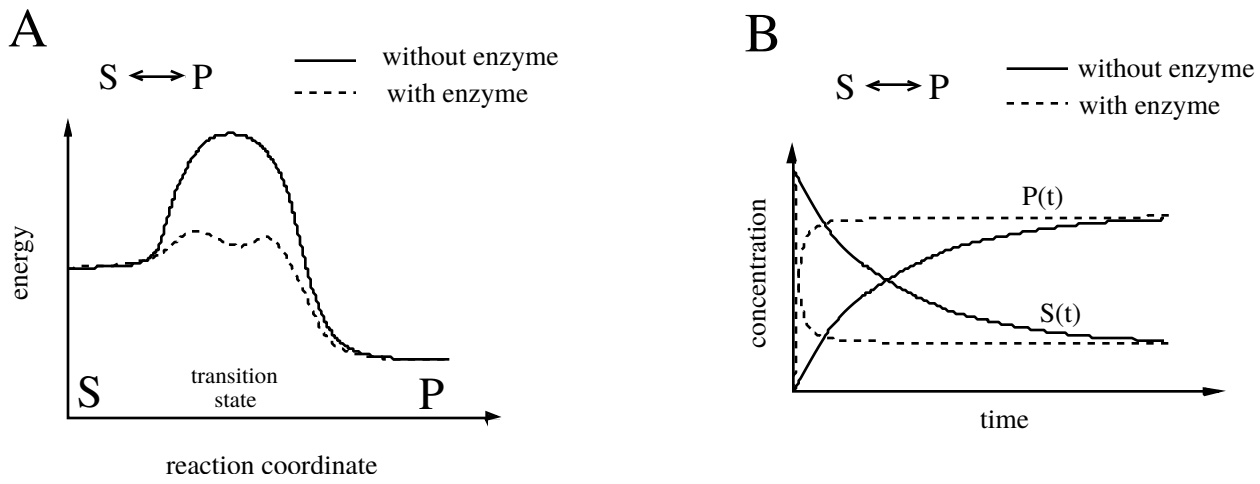

Figure 3.1: **A.** Effect of catalysis on reaction energy profile. Species P occupies a lower energy state than species S, so the equilibrium favors formation of P. For the reaction to occur, the reactants must collide with sufficient force to overcome the energy barrier (corresponding to formation of a high-energy transition state). Enzyme catalysis reduces the energy barrier between reactant and product. The enzyme does not affect the energy levels of the species themselves, and so has no effect on the equilibrium. **B.** Effect of catalysis on reaction dynamics. The ratio of concentrations at equilibrium depends only on the reactants S and P. The rate at which this equilibrium is attained is increased in the presence of an enzyme catalyst.

much as 10^7 times. The activity of enzymes within cells is highly regulated, through both genetic control of enzyme abundance and biochemical modification of individual enzyme molecules.

Experimental observations of enzyme-catalysed reactions show that they do not obey mass action rate laws. As sketched in Figure 3.2B, the rate of an enzyme-catalysed reaction approaches a limiting value as the substrate abundance grows. This saturating behaviour is caused by the fact that there is a limited amount of enzyme present: at high substrate concentrations, most of the enzymes are active, and so the addition of substrate has little effect on the reaction rate. The limiting reaction rate is reached when the entire enzyme pool is working at full capacity.

3.1.1 Michaelis-Menten kinetics

We will use model-reduction by time-scale separation to formulate a rate law that describes enzyme-catalyzed reactions. The first such derivation was made in 1913 by Leonor Michaelis and Maud Menten. The resulting rate law is called **Michaelis-Menten kinetics**.

The individual chemical events involved in a single-substrate enzyme-catalyzed reaction (Figure 3.2A) can be written as:

$$\underbrace{S}_{\text{substrate}} + \underbrace{E}_{\text{free enzyme}} \rightleftharpoons \underbrace{C_1}_{\text{enzyme-substrate complex}} \rightleftharpoons \underbrace{C_2}_{\text{enzyme-product complex}} \rightleftharpoons \underbrace{P}_{\text{product}} + \underbrace{E}_{\text{free enzyme}} \tag{3.1}$$

In our initial analysis, we will make two simplifications. Firstly, we will lump the two complexes C_1 and C_2 together, assuming that the time-scale of the conversion $C_1 \leftrightarrow C_2$ is fast compared to the timescale of the association and disassociation events. (This is a rapid equilibrium assumption.) Secondly, we will suppose that the product P never binds free enzyme. This makes the analysis simpler and is motivated by the fact that laboratory measurements of reaction rates are typically

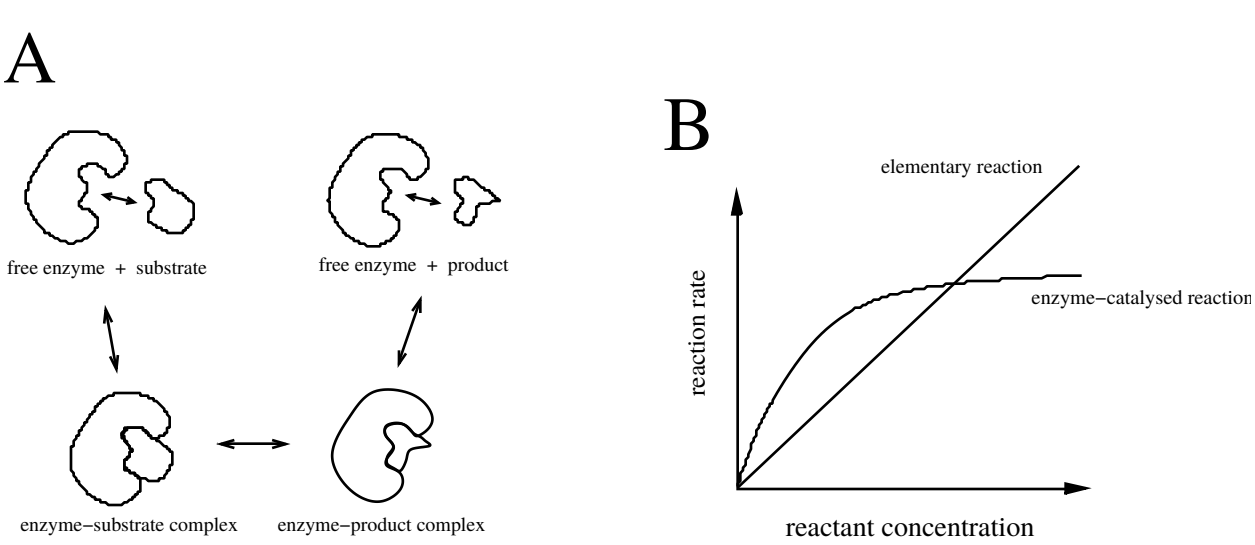

Figure 3.2: **A.** Lock-and-key model of the enzyme catalysis cycle. The substrate binds a specific site on the enzyme, called the active (or catalytic) site. Once bound, the enzyme facilities formation of the product. The product dissociates from the enzyme, which is then free to catalyse another reaction event. **B.** Rate laws for an enzyme-catalysed reaction and an elementary reaction. The mass action rate of the elementary reaction increases linearly with reactant concentration. In contrast, the rate of the enzyme-catalysed reaction tends to a limiting value as the reactant concentration grows.

carried out in the absence of product. The resulting rate law describes irreversible enzyme-catalysed reactions; the analogous rate law for reversible reactions will be presented later (equation (3.9)).

These two assumptions lead to the simplified network

$$S + E \underset{k_{-1}}{\overset{k_1}{\rightleftharpoons}} C \xrightarrow{k_2} P + E \tag{3.2}$$

The reaction rate k_2 is called the enzyme's *catalytic constant* (often denoted k_{cat}).

Applying the law of mass action, and denoting concentrations by s (substrate), e (free enzyme), c (complex), and p (product), we have the following differential equation model:

$$\begin{aligned}
\frac{d}{dt}s(t) &= -k_1 s(t)e(t) + k_{-1}c(t) \\
\frac{d}{dt}e(t) &= k_{-1}c(t) - k_1 s(t)e(t) + k_2 c(t) \\
\frac{d}{dt}c(t) &= -k_{-1}c(t) + k_1 s(t)e(t) - k_2 c(t) \\
\frac{d}{dt}p(t) &= k_2 c(t).
\end{aligned}$$

Let e_T denote the total enzyme concentration: $e_T = e + c$. Since the enzyme is not consumed in the reaction, e_T is constant—the enzyme is a conserved moiety. Writing $e(t) = e_T - c(t)$, we can use this conservation to eliminate the differential equation for $e(t)$, giving

$$\frac{d}{dt}s(t) = -k_1 s(t)(e_T - c(t)) + k_{-1}c(t)$$

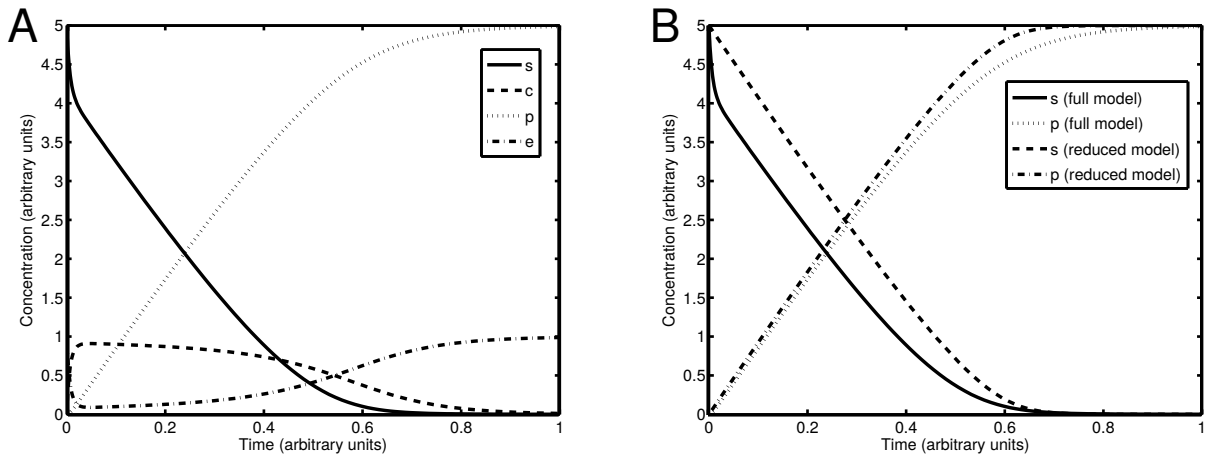

Figure 3.3: **A.** Simulation of enzyme catalysis. Model (3.3) is simulated with parameter values $k_1 = 30$ (concentration$^{-1} \cdot$ time^{-1}), $k_{-1} = 1$ (time^{-1}), $k_2 = 10$ (time^{-1}) and $e_T = 1$ (concentration). Initial concentrations are $s(0) = 5$, $c(0) = 0$, $p(0) = 0$. (Units are arbitrary.) A separation of time-scales is evident. On the fast time-scale, the complex C reaches a quasi-steady-state. The reaction $S \to P$ proceeds on the slower time-scale. **B.** Michaelis-Menten approximation of an enzyme-catalysed reaction $S \to P$. Model (3.3) (full model) is simulated as in panel A. The reduced model (3.4) provides a good approximation. The error in the approximation for S is caused by the sequestration of S into the complex C. In the cell, the ratio of substrate to enzyme molecules is typically much higher than in this simulation, so the sequestration effect is negligible.

$$\begin{aligned} \frac{d}{dt}c(t) &= -k_{-1}c(t) + k_1 s(t)(e_T - c(t)) - k_2 c(t) \\ \frac{d}{dt}p(t) &= k_2 c(t). \end{aligned} \tag{3.3}$$

(Although we won't need to, we could also use the conservation $s + c + p$ to further simplify the model formulation.)

A simulation of this model is shown in Figure 3.3A. The time-courses reveal a separation of time-scales. On the fast time-scale, substrate S and free enzyme E associate to form the complex C. On the slower timescale, S is converted to P. We will use this separation of time-scales for model reduction. Michaelis and Menten applied a rapid equilibrium approximation to the association/dissociation reaction ($S + E \leftrightarrow C$). We will present an alternative derivation developed by G. E. Briggs and J. B. S. Haldane* in 1925. (The rapid equilibrium derivation is treated in Exercise 3.1.1.)

The separation of time-scales evident in Figure 3.3A has two sources. The first is a difference in time constants for the reaction events ($\frac{1}{k_1+k_{-1}}$ for the association/dissociation $S + E \leftrightarrow C$, and $\frac{1}{k_2}$ for product formation $C \to P$). The second is a distinction in concentrations. For most metabolic reactions in the cell, the substrate is far more abundant than the enzyme ($s \gg e_T$). Consequently, the enzyme complexes quickly come to equilibrium *with respect to the more abundant substrate.*

*Haldane (1892-1964) made significant contributions to biology, and was one of the founders of the field of population genetics. His published essays are full of insight and wit. An accomplished naturalist, he was once asked what could be inferred about the mind of the Creator from the works of Creation. His response: "An inordinate fondness for beetles." (Beetles represent about 25% of all known animal species.)

(See problem 3.7.2 for details.) The complex C can thus be considered in quasi-steady state.

Recall that in its quasi-steady state, $c(t) = c^{qss}(t)$ is no longer an independent dynamic variable, but instead "tracks" the other variables in the system according to

$$0 = -k_{-1}c^{qss}(t) + k_1 s(t)[e_T - c^{qss}(t)] - k_2 c^{qss}(t).$$

Solving for $c^{qss}(t)$, we find

$$c^{qss}(t) = \frac{k_1 e_T s(t)}{k_{-1} + k_2 + k_1 s(t)}.$$

Substituting this quasi-steady-state expression into the model (3.3), we are left with:

$$\begin{aligned} \frac{d}{dt}s(t) &= -\frac{k_2 k_1 e_T s(t)}{k_{-1} + k_2 + k_1 s(t)} \\ \frac{d}{dt}p(t) &= \frac{k_2 k_1 e_T s(t)}{k_{-1} + k_2 + k_1 s(t)}. \end{aligned} \tag{3.4}$$

This reduced model describes $S \to P$ as a single (non-elementary) reaction. The reaction rate is called a **Michaelis-Menten rate law**. Figure 3.3B shows the behaviour of this reduced model in comparison to the original model (3.3).

Next, we define $V_{\max} = k_2 e_T$ as the *limiting (or maximal) rate* and $K_M = \frac{k_{-1}+k_2}{k_1}$ as the *Michaelis* (or *half-saturating*) *constant*, and write the rate law as

$$\text{rate of } S \to P = \frac{k_2 k_1 e_T s}{k_{-1} + k_2 + k_1 s} = \frac{V_{\max} s}{K_M + s}. \tag{3.5}$$

This rate law, sketched in Figure 3.4, is called *hyperbolic* (because the curve forms part of a hyperbola).

Exercise 3.1.1 Michaelis and Menten derived rate law (3.5) using a rapid equilibrium approximation applied to the association/disassociation of substrate and enzyme. Starting with scheme (3.2), follow this approach and re-derive the Michaelis-Menten rate law $V_{\max}s/(K_M + s)$. You will end up with a different formula for the Michaelis constant. Experimental characterizations of Michaelis-Menten rate laws involve direct measurement of K_M and $V_{\max}$, so the relation between K_M and the individual kinetic constants (k_1, k_{-1}, k_2) is not significant. □

Kinetic order

Recall that, as introduced in Section 2.1.2, when a reaction rate is given by mass action, the kinetic order of a reactant is the power to which that reactant's concentration is raised in the rate law. The notion of kinetic order can be generalized as follows. If s is the concentration of a substrate for a reaction with rate $v(s)$, then the kinetic order of s is

$$\text{kinetic order} = \left(\frac{s}{v}\right)\frac{dv}{ds}. \tag{3.6}$$

Using this definition, the kinetic order of the substrate s in the Michaelis-Menten rate law is

$$\left(\frac{s}{\frac{V_{\max}s}{K_M+s}}\right) \cdot \frac{d}{ds}\left(\frac{V_{\max}s}{K_M+s}\right) = \left(\frac{s(K_M+s)}{V_{\max}s}\right)\left(\frac{V_{\max}(K_M+s) - V_{\max}s}{(K_M+s)^2}\right) = \frac{K_M}{K_M+s} \tag{3.7}$$

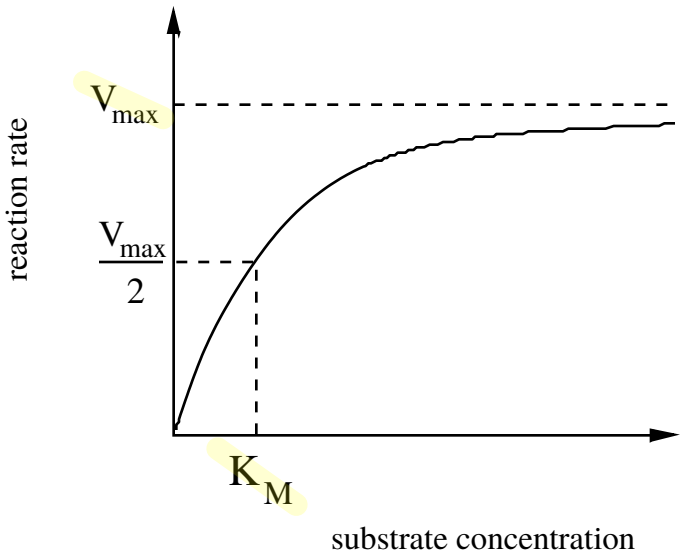

Figure 3.4: Michaelis-Menten rate law for a single-substrate enzyme-catalyzed reaction. The reaction rate approaches the limiting rate $V_{\max}$ as the substrate concentration increases. The Michaelis constant is the substrate concentration at which the rate is equal to half of the limiting rate.

In contrast with mass action, this kinetic order changes as the substrate concentration varies. In particular, when the concentration s is small compared to K_M, the kinetic order is roughly one (because $K_M + s \approx K_M$). Conversely, when s is large, the kinetic order is roughly zero. This is consistent with Figure 3.4. When s is near zero the curve grows linearly; when s is high, the curve is roughly horizontal (constant-valued). For small s, the enzyme is said to be operating in the *first-order* (or linear) regime, while for large s, the enzyme is saturated and is said to be acting in the *zero-order* regime.

Exercise 3.1.2 a) Apply the definition of kinetic order in equation (3.6) to the mass-action rate law $v(s) = ks^n$, and confirm that the result is consistent with the definition of kinetic order in Section 2.1.2.
b) When s is small, the Michaelis-Menten rate law is approximately linear. What is the slope of the corresponding linear relationship? That is, given that

$$\frac{V_{\max} s}{K_M + s} \approx ks$$

for s small, what is the corresponding constant k? □

Reversible reactions

When both substrate and product are present, the enzyme-catalysed reaction scheme is

$$S + E \underset{k_{-1}}{\overset{k_1}{\rightleftharpoons}} C \underset{k_{-2}}{\overset{k_2}{\rightleftharpoons}} P + E \tag{3.8}$$

Assuming the complex C is in quasi-steady-state with respect to S and P, the reaction rate (which can now take negative values) is given by the reversible Michaelis-Menten rate law:

$$\text{net rate of } S \to P \;=\; \frac{V_f \frac{s}{K_S} - V_r \frac{p}{K_P}}{1 + \frac{s}{K_S} + \frac{p}{K_P}}, \tag{3.9}$$

where V_f and V_r are the maximal rates of the forward and reverse reactions, and K_S and K_P are the Michaelis constants for S and P respectively (details in Problem 3.7.3). In some cases, the product re-binds to the free enzyme, but the rate of the reverse reaction is negligible. This is referred to as product inhibition (Problem 3.7.4).

Exercise 3.1.3 Verify the *Haldane relation*, which states that when the enzyme-catalysed reaction $S \leftrightarrow P$ is in equilibrium,

$$K_{eq} = \frac{p}{s} = \frac{k_1 k_2}{k_{-1} k_{-2}}.$$

(Hint: When $S \leftrightarrow P$ is in equilibrium, both of the reversible reactions in scheme (3.8) must be in equilibrium.) □

3.1.2 Two-substrate reactions

Most enzyme-catalysed reactions involve more than one substrate. To describe enzyme-catalysis of these reactions, we must expand our description of Michaelis-Menten kinetics.

Catalysis of the irreversible two-substrate reaction

$$A + B \;\to\; P + Q$$

involves two distinct association events: each substrate must bind the catalysing enzyme. (Trimolecular collisions in which both substrates bind the enzyme simultaneously are exceedingly rare events and so can be neglected.) The catalytic process can follow a number of different routes, including:*

- a *compulsory order* mechanism, in which substrate A binds to the free enzyme, thus forming a complex EA. Substrate B then binds, forming a ternary (i.e. three-molecule) complex EAB. This complex is then converted to EPQ, from which the products are released.

- a *random order* mechanism, in which either substrate can bind first. The products are released from the ternary complex EPQ.

- a *double-displacement* (or *ping-pong*) mechanism, in which substrate A first forms a complex EA with the enzyme. The enzyme is then modified in some manner (for example, by gaining a functional group from A), and product P is released. The modified enzyme E^* then binds B, forming complex E^*B. The enzyme recovers its original state by converting B to Q. Finally, product Q is released.

*Here we use concatenation of species names to denote molecular complexes. This is standard practise in biochemistry and is a useful notation, but unfortunately can be confused with the multiplicative product when these symbols are also used to represent concentrations. We will avoid such confusion by using distinct notation for chemical species and concentrations, e.g. $a = [A]$, $b = [B]$, so that AB is a molecular complex, while ab is the product of two concentrations.

To develop a two-substrate Michaelis-Menten rate law, consider the compulsory order reaction scheme

$$\begin{aligned} E + A &\underset{k_{-1}}{\overset{k_1}{\rightleftharpoons}} EA \\ EA + B &\underset{k_{-2}}{\overset{k_2}{\rightleftharpoons}} EAB \\ EAB &\xrightarrow{k_3} E + P + Q. \end{aligned} \tag{3.10}$$

As in the single-substrate case, a rate law can be derived by assuming that the complexes come to quasi-steady state. (This is justified if the substrates are abundant compared to the enzyme.)

Letting $C_1 = EA$, with concentration c_1, and $C_2 = EAB$, with concentration c_2, we can model the complexes by

$$\begin{aligned} \frac{d}{dt}c_1(t) &= k_1 a(t)e(t) - k_{-1}c_1(t) - k_2 c_1(t)b(t) + k_{-2}c_2(t) \\ \frac{d}{dt}c_2(t) &= k_2 c_1(t)b(t) - k_{-2}c_2(t) - k_3 c_2(t) \end{aligned}$$

Using conservation of enzyme to substitute for the free enzyme concentration ($e(t) = e_T - c_1(t) - c_2(t)$) and applying a quasi-steady-state approximation to both complexes gives a reaction rate of:

$$\text{rate of } A + B \to P + Q = k_3 c_2^{qss}(t) = \frac{k_3 e_T a(t)b(t)}{k_{-1}\frac{k_{-2}+k_3}{k_1 k_2} + \frac{k_{-2}+k_3}{k_2}a(t) + \frac{k_3}{k_1}b(t) + a(t)b(t)}. \tag{3.11}$$

Exercise 3.1.4 Verify Equation (3.11). □

This rate law the compulsory-order enzyme-catalysed reaction $A + B \to P + Q$ can be written more concisely as

$$v = \frac{V_{\max} ab}{K_{AB} + K_B a + K_A b + ab} \tag{3.12}$$

When the same technique is applied to the other reaction mechanisms described above (random order and double-displacement), similar reaction rates can be derived (Problem 3.7.6).

Note that if the concentration of either A or B is held constant, then this rate law reduces to a single-substrate Michaelis-Menten expression. This simplification is commonly used when one substrate is present at a near-fixed concentration, for example when it is a common co-reactant (called a *co-factor*), such as water or ATP. In those cases, a single-substrate Michaelis-Menten rate law is used, because the reaction is effectively dependent on a single reactant concentration.

Exercise 3.1.5 Consider rate law (3.12).
a) Verify that when the concentration of A is very high, the rate law reduces to a single-substrate Michaelis-Menten rate law for B, with maximal rate $V_{\max}$ and Michaelis constant $K_M = K_B$. Verify that this is consistent with the limiting behaviour of the reaction network (3.10) (which in this case takes the form $EA + B \leftrightarrow EAB \to EA + P + Q$, because all enzyme will be continually bound to A.)

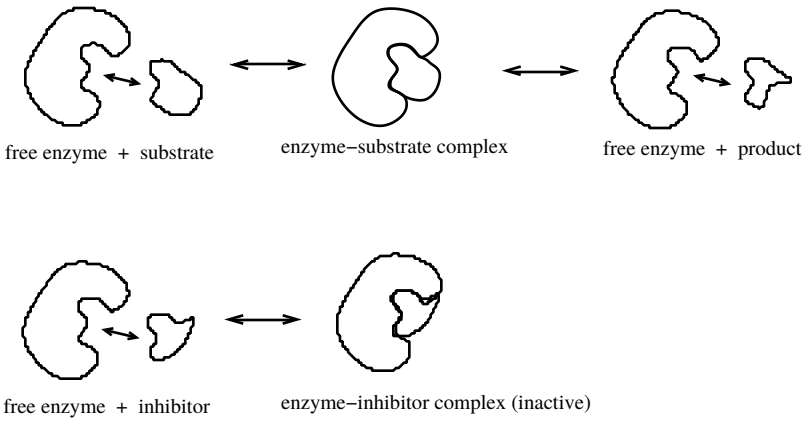

Figure 3.5: Competitive inhibition of enzyme catalysis. The inhibitor—a chemical mimic of the substrate—binds the enzyme's active site. Inhibitor-bound enzymes are not available to catalyse reactions.

b) Verify that when the concentration of B is very high, the rate law reduces to a single-substrate Michaelis-Menten rate law for A, with maximal rate $V_{\max}$ and Michaelis constant $K_M = K_A$. Verify that this is consistent with the limiting behaviour of the reaction network (3.10) (which in this case takes the form $E + A \to EAB \to E + P + Q$, because complex EA will bind B immediately after forming.) □

3.2 Regulation of Enzyme Activity

Enzyme activity can be regulated through a number of mechanisms. Genetic effects can cause changes in the abundance of enzymes (e_T in our models). These changes occur on the slow time-scale of genetic processes—minutes to hours. A much faster means of control is provided by biochemical modification of individual enzyme molecules. We will consider two distinct mechanisms by which enzyme activity can be altered biochemically: competitive inhibition and allosteric regulation.

3.2.1 Competitive inhibition

A competitive inhibitor is a molecule that mimics an enzyme's substrate, but does not undergo a reaction, as shown in Figure 3.5. This impostor molecule binds to the active site and clogs the enzyme so it is not available for catalysis. (A familiar example is the drug aspirin; it binds the active site of the enzyme cyclooxygenase and thus inhibits the production of prostoglandins, which are involved in pain pathways, blood clotting, and production of stomach mucus.)

To derive a rate law for a competitively inhibited enzyme, we construct a reaction scheme consisting of both the catalytic process and the formation of an enzyme-inhibitor complex.

$$S + E \underset{k_{-1}}{\overset{k_1}{\rightleftharpoons}} C \xrightarrow{k_2} E + P$$

$$I + E \underset{k_{-3}}{\overset{k_3}{\rightleftharpoons}} C_I,$$

where I is the inhibitor and C_I is the inactive enzyme-inhibitor complex. We will apply a quasi-steady-state approximation to the two complexes. With c and c_I denoting concentrations, we have

$$\begin{aligned} \frac{dc}{dt} &= k_1 s(t) e(t) - k_{-1} c(t) - k_2 c(t) \\ \frac{dc_I}{dt} &= k_3 e(t) i - k_{-3} c_I(t). \end{aligned}$$

We treat the inhibitor concentration i as a fixed quantity. (This is justified by presuming that the inhibitor is far more abundant than the enzyme, so that formation of C_I does not change i significantly.) Applying the quasi-steady state assumption to the two complexes and employing the conservation $e(t) = e_T - c(t) - c_I(t)$ yields

$$c = \frac{e_T s}{\frac{iK_M}{K_i} + s + K_M} \tag{3.13}$$

where $K_M = \frac{k_{-1}+k_2}{k_1}$ and K_i is the *dissociation constant* for inhibitor binding: $K_i = \frac{k_{-3}}{k_3}$. The rate law can then be written as

$$\text{rate of } S \to P \;=\; k_2 c = \frac{V_{\max} s}{K_M(1 + i/K_i) + s},$$

with $V_{\max} = k_2 e_T$.

This rate law is sketched in Figure 3.6 for various levels of inhibitor. Competitive inhibition does not influence the limiting reaction rate $V_{\max}$. When the substrate is much more abundant than the inhibitor, the inhibition has only a negligible effect. However, the competition for enzymes affects the concentration of substrate needed to achieve a given reaction rate: the effective Michaelis constant of the inhibited reaction, $K_M(1 + i/K_i)$, increases with inhibitor abundance.

Exercise 3.2.1 Verify equation (3.13). □

Competitive inhibition depends on the conformation of the enzyme's active site; inhibitors must be chemically similar to reactants. We next consider a more versatile form of regulation that does not suffer from this restriction and instead employs components of the regulated enzyme besides the active site.

3.2.2 Allosteric regulation

The catalytic efficiency of an enzyme depends on the conformation of its active site. This conformation depends, in turn, on the overall configuration of the protein (its tertiary structure). This configuration, and hence the nature of the active site, can be altered by modifications to the chemical energy landscape of the protein, e.g. the position and strength of charges. Such modifications can be made by molecules that bind the protein. This mode of enzyme regulation, called **allosteric control**, was proposed by François Jacob and Jacques Monod in 1961. The term 'allostery' (from Greek, *allo*: other, *steros*: solid, or shape) emphasizes the distinction from competitive inhibition—the regulating molecule need not bear any chemical resemblance to the substrate. Likewise, the site on the enzyme where the regulator binds (called the *allosteric site*) can be distinct from the active site in both position and chemical structure.

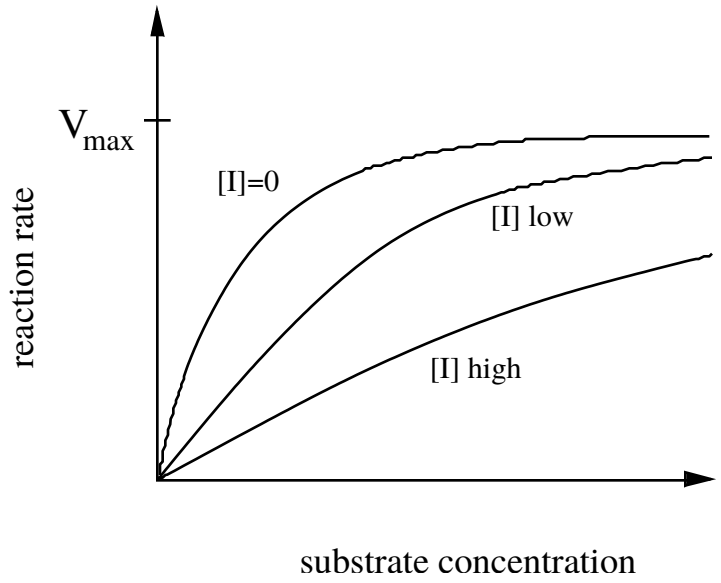

Figure 3.6: Reaction rates for competitively inhibited enzyme catalysis. The limiting reaction rate, $V_{\max}$, is unaffected by the presence of the inhibitor. Instead, the inhibitor increases the substrate concentration required to reach the half-maximal rate.

Typically, the binding of an allosteric regulator to a protein invokes a transition between a functional state and a non-functional state. For enzymes, this a transition between a catalytically active form and an inactive form.

Allosteric effects offer a range of strategies for the regulation of enzyme activity. For instances, conformational changes can affect substrate binding or reaction catalysis. Moreover, an enzyme molecule might simultaneously bind multiple allosteric regulators whose effects can be integrated in a variety of ways. In this section we will consider a simple case that highlights the functional differences between allosteric inhibition and competitive inhibition.

Consider an enzyme that binds a single allosteric regulator. Suppose the regulator inhibits enzyme catalysis by blocking product formation, as shown in Figure 3.7. For simplicity, we will assume that the inhibitor has no effect on substrate binding. The reaction scheme is

$$\begin{aligned} S + E &\underset{k_{-1}}{\overset{k_1}{\rightleftharpoons}} ES \xrightarrow{k_2} E + P \\ I + E &\underset{k_{-3}}{\overset{k_3}{\rightleftharpoons}} EI \\ I + ES &\underset{k_{-3}}{\overset{k_3}{\rightleftharpoons}} ESI \\ S + EI &\underset{k_{-1}}{\overset{k_1}{\rightleftharpoons}} ESI \end{aligned} \tag{3.14}$$

We have assumed that the binding of substrate and inhibitor are independent. This scheme is called *non-competitive inhibition.*

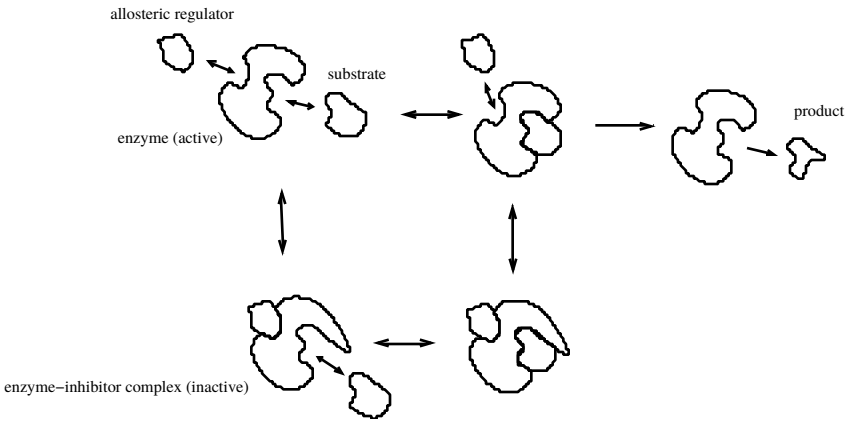

Figure 3.7: Allosteric inhibition of enzyme activity. The enzyme has two binding sites: the active site where the substrate binds, and the allosteric site where the allosteric regulator binds. In this example, the inhibited enzyme can bind substrate, but cannot catalyse formation of the reaction product.

To derive a rate law, the quasi-steady state approximation can be applied to the complexes ES, EI and ESI. Together with the conservation $e_T = [E] + [ES] + [EI] + [ESI]$, this gives the reaction rate as:

$$\text{rate of } S \to P \;=\; k_2[ES] = \frac{V_{\max}}{1 + i/K_i} \frac{s}{K_M + s} \tag{3.15}$$

where $V_{\max} = k_2 e_T$, $K_M = \frac{k_{-1}+k_2}{k_1}$ and $K_i = \frac{k_{-3}}{k_3}$. This rate law is sketched in Figure 3.8 for various levels of inhibitor. In contrast with competitive inhibition, this allosteric inhibitor reduces the limiting rate $V_{\max}$, but does not affect the half-saturating concentration K_M. More generally, other allosteric inhibition schemes impact both $V_{\max}$ and K_M.

Exercise 3.2.2 An alternative to the non-competitive inhibition scheme of Figure 3.7 is *uncompetitive inhibition*, in which the inhibitor only binds the enzyme-substrate complex (so complex EI does not occur). Apply a quasi-steady-state analysis to verify that uncompetitive inhibition reduces K_M and $V_{\max}$ by the same factor. □

3.3 Cooperativity

The term **cooperativity** is used to describe potentially independent binding events that have a significant influence on one another, leading to nonlinear behaviours. The most commonly cited example (and the first to be recognized, at the turn of the 20th century) is oxygen-binding to the protein *hemoglobin*. Hemoglobin is the main transporter of oxygen in blood (in vertebrates). Hemoglobin is a tetrameric protein (i.e. composed of four polypeptide chains); each monomer binds one oxygen molecule.

Hemoglobin's efficiency as an oxygen carrier can be assessed by a curve showing the fraction of protein in the oxygen-bound form as a function of the abundance of oxygen. When these plots were first generated from experimental data, the binding curve for hemoglobin was found to have an S-shaped, or *sigmoidal* character, as sketched in Figure 3.9. This came as somewhat of a surprise, as most binding curves are hyperbolic, not sigmoidal.

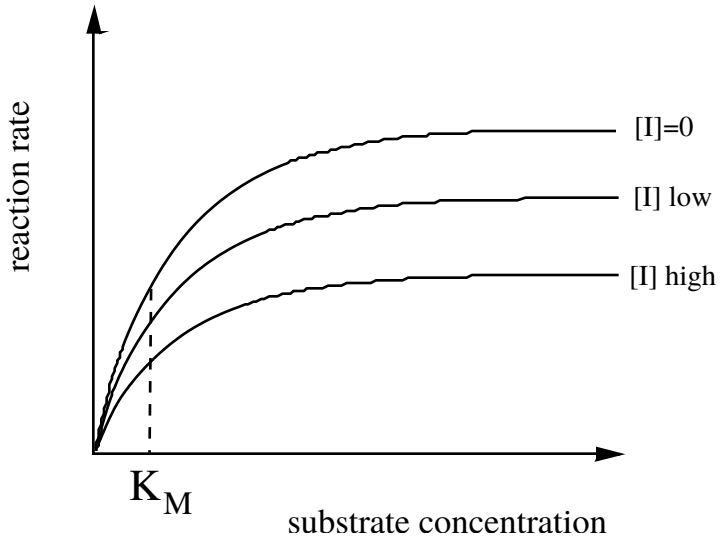

Figure 3.8: Rate laws for allosterically inhibited enzyme catalysis (non-competitive inhibition). The limiting reaction rate is reduced by the inhibitor. The binding affinity, reflected in the half-maximal substrate concentration K_M, is unaffected.

Further insight into the oxygen-binding behaviour of hemoglobin came from studies of the closely related protein myoglobin, which is used to store oxygen in vertebrate muscle cells. Structurally, myoglobin is very similar to the individual monomers that form a hemoglobin tetramer. As shown in Figure 3.9, the binding curve for myoglobin is hyperbolic. This suggests that hemoglobin's sigmoidal binding curve does not result from the nature of the individual binding sites. Rather, this nonlinearity results from cooperative interactions among the four monomers.

To address cooperativity, consider the binding of a molecule X to a protein P. The generic name for a binding molecule is **ligand** (from Latin, *ligare*: to bind). The reaction scheme is

$$P + X \underset{k_{-1}}{\overset{k_1}{\rightleftharpoons}} PX \tag{3.16}$$

The *fractional saturation* of the pool of proteins, denoted Y, is defined as the fraction of binding sites that are occupied by ligand:

$$Y = \frac{\text{number of occupied binding sites}}{\text{total number of binding sites}} = \frac{[PX]}{[P] + [PX]}.$$

Letting $K = \frac{k_{-1}}{k_1}$ (the dissociation constant for the binding event), we find, at steady state, $[PX] = [P][X]/K$. Then we have

$$Y = \frac{[P][X]/K}{[P] + [P][X]/K} = \frac{[X]/K}{1 + [X]/K} = \frac{[X]}{K + [X]}. \tag{3.17}$$

(This functional form was seen earlier in the Michaelis-Menten rate law; the rate of an enzyme-catalysed reaction is proportional to the fractional occupancy of the enzyme.)

The binding curve associated with equation (3.17) is hyperbolic—consistent with the oxygen-binding behaviour of myoglobin. To describe the binding of oxygen to hemoglobin, we will next consider a protein P with four ligand-binding sites.

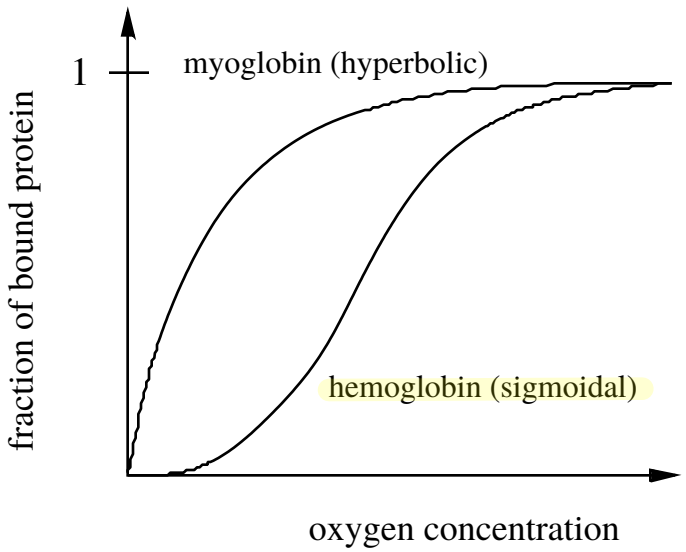

Figure 3.9: Binding curves for hemoglobin and myoglobin. Myoglobin shows a commonly observed hyperbolic behaviour. The binding curve for hemoglobin is *sigmoidal* (S-shaped). This nonlinear behaviour is characteristic of cooperative binding mechanisms.

If the binding sites are identical and the binding events are independent of one another, then the binding behaviour is no different from equation (3.17). (In this case, the tetrameric structure simply increases the number of independent binding sites per protein.) Likewise, if the binding events are independent and the binding sites have different affinities, then the binding curve is again hyperbolic (Problem 3.7.9).

To address the case in which the binding sites are identical but cooperative effects occur between them, consider the following scheme:

$$\begin{aligned} P + X &\underset{k_{-1}}{\overset{4k_1}{\rightleftharpoons}} PX_1 \\ PX_1 + X &\underset{2k_{-2}}{\overset{3k_2}{\rightleftharpoons}} PX_2 \\ PX_2 + X &\underset{3k_{-3}}{\overset{2k_3}{\rightleftharpoons}} PX_3 \\ PX_3 + X &\underset{4k_{-4}}{\overset{k_4}{\rightleftharpoons}} PX_4, \end{aligned}$$

where complex PX_i has i ligand molecules bound. The rate constants depend on the number of bound ligand molecules, as follows. The first association reaction has rate k_1, the second has rate k_2, and so on. These rate constants are scaled by stoichiometric pre-factors that account for the number of binding sites involved in each reaction. (For instance, there are four sites available for the first ligand to bind, so the overall reaction rate is $4k_1$. There are only three sites available for the second ligand to bind, so the rate is $3k_2$.)

Because there are four binding sites on each protein molecule, the fractional saturation is given

by

$$Y = \frac{\text{number of occupied binding sites}}{\text{total number of binding sites}} = \frac{[PX_1] + 2[PX_2] + 3[PX_3] + 4[PX_4]}{4([P] + [PX_1] + [PX_2] + [PX_3] + [PX_4])}$$

When the binding events are in equilibrium, the fractional saturation can be written as

$$Y = \frac{[X]/K_1 + 3[X]^2/(K_1K_2) + 3[X]^3/(K_1K_2K_3) + [X]^4/(K_1K_2K_3K_4)}{1 + 4[X]/K_1 + 6[X]^2/(K_1K_2) + 4[X]^3/(K_1K_2K_3) + [X]^4/(K_1K_2K_3K_4)}, \tag{3.18}$$

where the parameters K_i are the dissociation constants ($K_i = \frac{k_{-i}}{k_i}$, for $i = 1, 2, 3, 4$). This is known as the *Adair equation* for four sites. It exhibits a sigmoidal character when the affinities of the later binding events are significantly greater than those of the earlier events. This is positive cooperativity: the binding of the first ligand molecules enhance the binding of the remaining ligands.

If the final binding event has a much higher affinity than the earlier binding events (i.e. $K_4 \ll K_1, K_2, K_3$), then the fractional saturation can be approximated by

$$Y \approx \frac{[X]^4/(K_1K_2K_3K_4)}{1 + [X]^4/(K_1K_2K_3K_4)}.$$

This approximation is formalized in the **Hill function**

$$Y = \frac{([X]/K)^n}{1 + ([X]/K)^n} = \frac{[X]^n}{K^n + [X]^n}, \tag{3.19}$$

which is used to describe processes that involve multiple near-simultaneous binding events. The constant K is the half-saturating concentration of ligand, and so can be interpreted as an averaged dissociation constant. (Note that when $n = 1$ the Hill function reduces to a hyperbolic function.)

In 1910 the English physiologist A. V. Hill proposed the function (3.19) as a convenient curve for fitting the sigmoidal binding behavior observed for hemoglobin. Hill did not attach any significance to the particular form of this function—he used it as an empirical fit to the data.

As shown in Figure 3.10, the exponent n, called the *Hill coefficient*, reflects the steepness of the sigmoid, and is commonly used as a measure of the switch-like character of a process. The Hill coefficient is often chosen to coincide with the number of events in a multiple-binding-event process, as in our derivation above. However, Hill functions constructed in this manner must be interpreted carefully, since empirical observations often correspond to Hill coefficients well below the number of binding events. For example, Hill himself found that the hemoglobin binding data was best fit with values of n ranging from 1 to 3.2. (When fit to empirical data, non-integer Hill coefficients are commonly used.)

Having justified the difference in binding behaviour between myoglobin and hemoglobin, we can now interpret their respective biological functions. Myoglobin serves to *store* oxygen in muscle tissue, and so is saturated with oxygen at all but the lowest oxygen concentrations. Hemoglobin *shuttles* oxygen and so must bind and release oxygen in the appropriate conditions. A sigmoidal binding curve has the property that a relatively small change in ligand concentration can lead to a large change in binding saturation. This allows hemoglobin to fulfill its transport task without demanding a wide difference in oxygen concentrations at its 'pick up' and 'drop off' points. For example, the difference in oxygen concentration between the alveoli of the lungs and the capillaries of active muscle is only five-fold. A hyperbolic binding curve cannot exhibit a wide change in

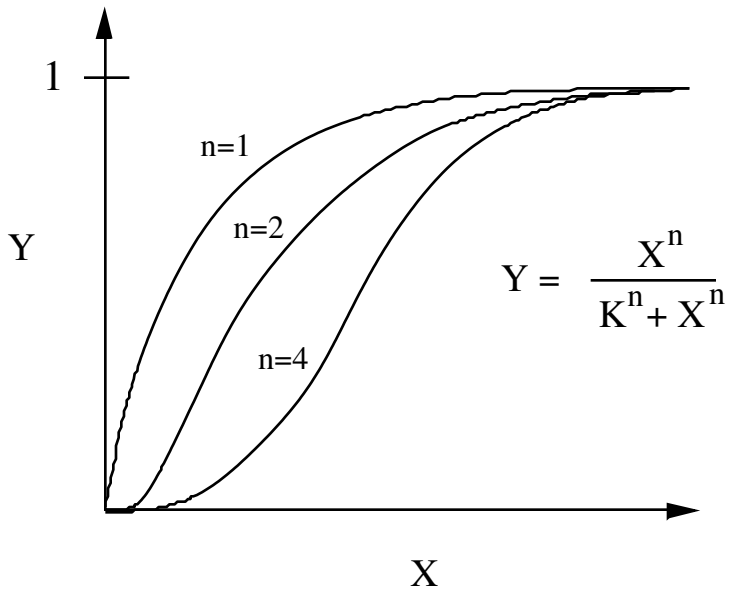

Figure 3.10: Hill functions. As the Hill coefficient n increases, the sigmoidal curve becomes more switch-like. When the Hill coefficient is 1, the curve is hyperbolic.

ligand binding over such a narrow range in ligand availability. (Indeed, an 81-fold change in ligand concentration is needed to take a hyperbolic binding curve from 10% to 90% saturation.) Cooperative binding provides hemoglobin with a narrow, *switch-like* response to oxygen availability, resulting in efficient shuttling. In subsequent chapters we will see a range of biological uses for such switch-like behaviour.

Exercise 3.3.1 Consider a protein that binds ligand at two identical sites and derive the corresponding Adair equation:

$$Y = \frac{[X]/K_1 + [X]^2/(K_1K_2)}{1 + 2[X]/K_1 + [X]^2/(K_1K_2)},$$

where K_1 and K_2 are the dissociation constants for the first and second binding events. □

Exercise 3.3.2 Verify that the Hill function (3.19) has slope $\frac{n}{4K}$ at its half saturation point ($[X] = K$). □

Exercise 3.3.3 The Hill function description of cooperative binding can be equivalently derived in the limiting case where n ligands bind protein P simultaneously. Confirm this fact by deriving the fractional saturation when the binding event is

$$P + nX \underset{k_{-1}}{\overset{k_1}{\rightleftharpoons}} PX_n.$$

The Hill function (3.19) can be recovered by setting $K = \sqrt[n]{k_{-1}/k_1}$. □

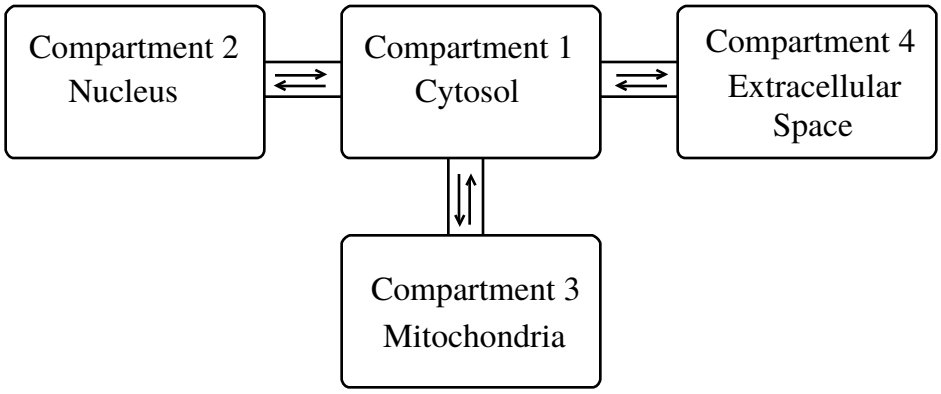

Figure 3.11: A multi-compartment model. Each compartment is presumed well-mixed. Transport between compartments is restricted to the connections shown. When multiple copies of a compartment are present (e.g. mitochondria), they can be treated as a single 'averaged' compartment.

Exercise 3.3.4 Consider an enzyme that has two identical catalytic sites, and suppose that the substrates exhibit cooperative binding. To simplify your analysis, presume that the cooperativity is strong, so that the substrates can be assumed to bind simultaneously (as in Exercise 3.3.3). Furthermore, presume that catalysis only occurs when two substrate molecules are bound. The reaction scheme is then

$$2S + E \underset{k_{-1}}{\overset{k_1}{\rightleftharpoons}} C \xrightarrow{k_2} 2P + E.$$

Verify that, in the absence of product, the reaction rate takes the form

$$v = \frac{V_{\max} s^2}{K_M + s^2}.$$

□

3.4 Compartmental Modelling and Transport

As described in Chapter 2, ordinary differential equation models rely on the assumption that the reaction network occurs in a well-stirred volume. The cell is, of course, not a homogeneous mixture, but this well-stirred assumption can often be justified when applied to individual cellular *compartments*. Prokaryotic cells typically consist of a single compartment, but eukaryotic cells are composed of a collection of membrane-bound compartments, e.g. mitochondria, the nucleus, the endoplasmic reticulum, and the cytosol.

Multi-compartment models can be used to describe systems that involve activity in more than one cellular compartment (Figure 3.11). In such models, species concentrations in each well-mixed compartment are described separately. Transport of molecules between connected compartments is described explicitly. In this section, we will consider some common models of cross-membrane transport.

3.4.1 Diffusion

Some molecules, such as oxygen, readily diffuse across bilipid membranes. The transport of such species can be described by *Fick's Law*, which states that the rate of diffusion is proportional to the difference in concentration.

To illustrate, suppose species S is present in two neighbouring compartments, and diffuses freely across the membrane that separates them. If $[S]_1$ and $[S]_2$ are the concentrations of S in compartments 1 and 2, then the rate of flow of molecules from compartment 1 to compartment 2 is given by

$$\text{rate of flow} = D([S]_1 - [S]_2) \tag{3.20}$$

where the constant D quantifies how readily S diffuses across the membrane. To describe the resulting changes in concentration, compartment volumes must be taken into account. If V_1 and V_2 are the volumes of compartments 1 and 2 respectively, the concentrations in the two compartments can be described by

$$\frac{d}{dt}[S]_1(t) = -\frac{D([S]_1(t) - [S]_2(t))}{V_1} \qquad \frac{d}{dt}[S]_2(t) = \frac{D([S]_1(t) - [S]_2(t))}{V_2}.$$

The constant D thus has units of volume $\cdot$ time^{-1}.

In the long-term, diffusion leads to equal concentrations in both compartments. The concentration in the smaller volume will approach steady state more quickly. In particular, if one compartment has a much larger volume than the other, the change in concentration in the larger compartment may be negligible, so it could be treated as a fixed pool (Problem 3.7.12).

Many molecular species, such as charged ions and macromolecules, cannot diffuse through bilipid membranes. Transport of these molecules is facilitated by specialized transporter proteins. In some cases, these proteins simply provide small holes in the membrane that allow particular molecular species to pass; these are called *channels*, or *pores*. For example, nuclear pores allow free diffusion of some species between the nucleus and cytosol of eukaryotic cells. Another example, ion-specific channels, will be taken up in Chapter 8. Transport through a channel or pore is drive by diffusion; the rate of transport is described by equation (3.20). (In this case, the coefficient D is proportional to the number of channels or pores that appear in the membrane.)

We next consider more specialized transporter proteins.

3.4.2 Facilitated transport

Many molecular species are transported across membranes in a species-specific fashion. Transmembrane carrier proteins bind specific molecules and facilitate their transport across the membrane, as in Figure 3.12.

Passive Transport

In some cases, the transport mechanism is reversible; the direction of transport is then determined by the concentration of ligand on either side of the membrane. This is called *facilitated diffusion* or *passive transport*, and results, in the long term, in equal concentrations in the two compartments.

Passive transport is similar to enzyme catalysis—instead of changing a molecule's chemical identity, a transporter "catalyses" a change in its location. A reaction scheme showing the steps in

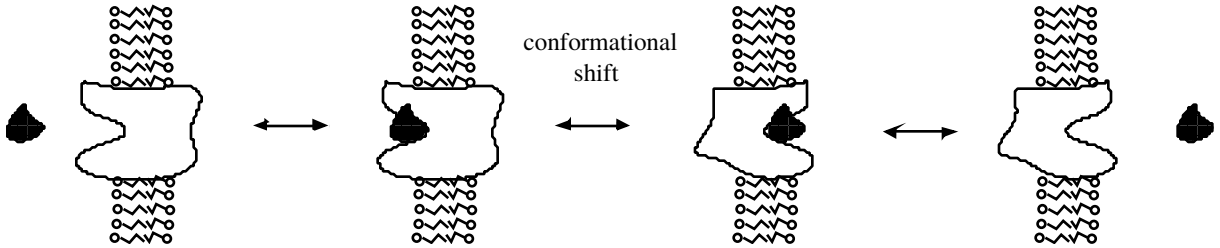

Figure 3.12: Transmembrane carrier protein. The ligand binds the protein on one side of the membrane. Through a conformational shift, the protein passes the ligand across the membrane and then releases it.

passive transport is identical to the scheme for a reversible enzyme-catalysed reaction:

$$S_1 + T \rightleftharpoons TS_1 \rightleftharpoons TS_2 \rightleftharpoons T + S_2$$

where T is the transporter and S_i is the transported species in compartment i.

If we make the simplifying assumption that the transport step ($TS_1 \leftrightarrow TS_2$) is in rapid equilibrium and then apply a quasi-steady-state approximation to the transporter-ligand complex, the rate of transport is given as:

$$\text{transport rate } = \frac{\alpha_1[S_1]/K_1 - \alpha_2[S_2]/K_2}{1 + [S_1]/K_1 + [S_2]/K_2},$$

where the parameters α_i are the maximal transport rates in each direction and the K_i reflect the binding affinities of the ligand on either side of the membrane. (Compare with equation (3.9).) This transport rate reduces to a linear expression ($\frac{\alpha_1}{K_1}[S_1] - \frac{\alpha_2}{K_2}[S_2]$) when the transporter pool is far from saturation (i.e. $[S_1] \ll K_1$ and $[S_2] \ll K_2$.)

This model describes a *uniporter*—a transporter that carries a single ligand molecule across a membrane. Other proteins transport multiple ligands simultaneously. Proteins that facilitate the transport of multiple ligands in the same direction are called *symporters*; simultaneous transport of ligands in opposite directions is facilitated by *antiporters*.

Exercise 3.4.1 Prepare a reaction scheme that corresponds to a two-ligand symporter. How does this mechanism compare with our treatment of two-substrate enzyme-catalysed reactions in Section 3.1.2? Does the analysis have to be modified to address a two-ligand antiporter? □

Active Transport

Passive diffusion acts to eliminate differences in concentration. In some cases, cellular processes maintain concentration gradients across membranes. In order to achieve these persistent gradients, cells expend energy to transport molecules against diffusion—from low concentration to high concentration—by *active transport*. Many active transporters, or *pumps*, consume ATP; others are co-transporters that couple the diffusion-driven transport of one molecule to the transport of another molecule against diffusion.

Because intracellular ATP levels are tightly regulated, models often treat the concentration of ATP as fixed. In these cases, the dependence of a transporter on ATP can be incorporated into an effective kinetic constant. Some pumps couple the consumption of a single ATP molecule to the transport of multiple ligand molecules. For example, the sodium-potassium pump, found in animal

cells, couples the consumption of a single ATP molecule to the transport of three Na^+ ions into the cell and two K^+ ions out of the cell, both against their respective concentration gradients.

Another example is provided by the Ca^{2+} pumps in the membrane of the endoplasmic reticulum of eukaryotic cells. Some of these pumps transport two Ca^{2+} ions out of the cytosol each time they consume an ATP molecule. Assuming that the two calcium ions bind near-simultaneously (i.e. with high cooperativity), and that the rate of transport is proportional to the fractional occupancy of the pumps, the transport rate is then

$$\text{transport rate} = \frac{\alpha[Ca^{2+}]^2}{K + [Ca^{2+}]^2} \tag{3.21}$$

where the maximal rate α is implicitly dependent on both the cytosolic ATP level and the abundance of pump proteins.

Exercise 3.4.2 Derive formula (3.21). (Compare with Exercise 3.3.4.) □

3.5 *Generalized Mass Action and S-System Modelling

The law of mass action provides an excellent description of reaction rates in ideal conditions: dilute molecular solutions at high molecule counts in a well-stirred reaction vessel. The rates of chemical processes occurring within the cell—a highly concentrated and inhomogeneous environment—often differ from mass action. These differences can sometimes be accounted for by describing reaction rates as functions of chemical *activities*, rather than concentrations. Chemical activities correspond to effective concentrations; they are dependent on the composition of the solution in which the reaction occurs. In some cases, the activity, a, is related to the concentration by a power-law: e.g. $a_X = [X]^\gamma$, for some exponent γ. Applying the law of mass action to these activities (instead of to concentrations) can give rate laws with non-integer powers of concentrations, e.g.

$$X \xrightarrow{k_1} Y \qquad \text{reaction rate}: \; k_1 a_X = k_1[X]^\gamma$$

$$X + X \xrightarrow{k_2} Z \qquad \text{reaction rate}: \; k_2(a_X)^2 = k_2([X]^\gamma)^2 = k_2[X]^{2\gamma}.$$

These are referred to as *Generalized Mass Action* (GMA) rate laws.

Generalizing mass action in this way allows simple approximations of complex rate laws. As an example, Figure 3.13 compares the generalized mass action rate law $v = s^{0.4}$ to the Michaelis-Menten rate law $v = \frac{2s}{1+s}$. The two curves agree quite well over the range shown, although they diverge for larger values of the substrate concentration. (The GMA rate law does not saturate.) In this simple case, we generally prefer the Michaelis-Menten formulation since it was derived from the reaction mechanism, while the GMA rate law can only be used as an empirical fit. However, when more complex rate laws are considered—especially those involving multiple substrates and regulators—the GMA approximation becomes more attractive. The number of parameters in a Michaelis-Menten rate law increases rapidly as more substrates or regulators are included in the reaction mechanism. In contrast, a GMA formulation involves about one parameter per species, and so provides a formulation that is much more tractable in terms of fitting to experimental data.

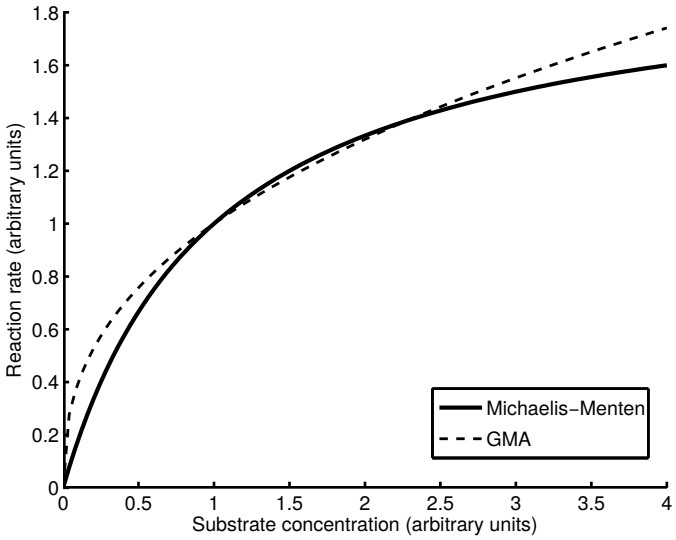

Figure 3.13: Comparison of generalized mass action and Michaelis-Menten rate laws. The GMA rate law ($v = s^{0.4}$) provides a good approximation to the Michaelis-Menten rate law ($v = \frac{2s}{1+s}$) over the range shown, but diverges as the substrate concentration increases.

S-system modelling

In the late 1960's Michael Savageau proposed a novel modelling framework the takes the simplification inherent in a GMA formulation one step further. Savageau's approach condenses each differential equation in a model by lumping all production terms into a single GMA expression, and all consumption terms into another. The result is a simple model that contains relatively few parameters and yet is able to describe a wide range of nonlinear behaviours. Models of this type have come to be called *S-system models*. (The "S" stands for synergism and saturation. S-system modelling provides a simple framework for approximating these nonlinear effects.)

One significant advantage of the S-system framework is that the steady-state species concentrations can always be determined analytically—after a transformation, the steady-state solution can be found by solving a linear system of equations. In contrast, Michaelis-Menten formulations rarely give rise to systems for which the steady state be described explicitly.

To illustrate the S-system modelling framework, consider the reaction scheme shown in Figure 3.14, in which species S_2 allosterically inhibits its own production. The concentrations s_1 and s_2 of species S_1 and S_2 satisfy

$$\begin{aligned} \frac{d}{dt}s_1(t) &= v_1 - v_2 \\ \frac{d}{dt}s_2(t) &= v_2 - v_3 - v_4. \end{aligned} \tag{3.22}$$

To construct an S-system model, we make the following power-law approximations:

$$v_1 = \alpha_1 \qquad v_2 = \alpha_2 s_1^{g_1} s_2^{g_2} \qquad v_3 + v_4 = \alpha_3 s_2^{g_3} \tag{3.23}$$

The parameters α_i are rate constants; the g_i are kinetic orders. Because S_2 acts as an allosteric inhibitor, g_2 will be negative.

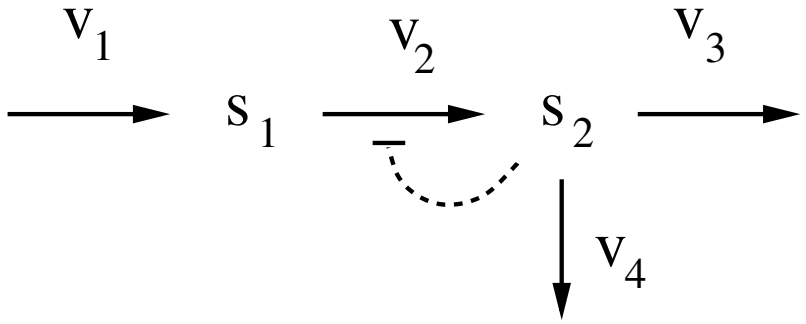

Figure 3.14: Reaction scheme for S-system model analysis. The labels v_i indicate the rates of the corresponding reactions. (They are not mass action rate constants.)

The steady-state species concentrations satisfy

$$\begin{aligned} 0 &= \alpha_1 - \alpha_2 s_1^{g_1} s_2^{g_2} \\ 0 &= \alpha_2 s_1^{g_1} s_2^{g_2} - \alpha_3 s_2^{g_3}. \end{aligned}$$

These equations can be rewritten as

$$\begin{aligned} \alpha_1 &= \alpha_2 s_1^{g_1} s_2^{g_2} \\ \alpha_2 s_1^{g_1} s_2^{g_2} &= \alpha_3 s_2^{g_3}. \end{aligned}$$

The terms in these equations are all positive, allowing us to take logarithms. The logarithm of the first equation gives

$$\log \alpha_1 = \log(\alpha_2 s_1^{g_1} s_2^{g_2}) = \log \alpha_2 + \log s_1^{g_1} + \log s_2^{g_2} = \log \alpha_2 + g_1 \log s_1 + g_2 \log s_2.$$

The second equation yields

$$\log \alpha_2 + g_1 \log s_1 + g_2 \log s_2 = \log \alpha_3 + g_3 \log s_2.$$

This is a pair of linear equations in $\log s_1$ and $\log s_2$; it can be solved to yield

$$\begin{aligned} \log s_1 &= \frac{\log \alpha_1 - \log \alpha_2 - \frac{g_2}{g_3}(\log \alpha_1 - \log \alpha_3)}{g_1} \\ \log s_2 &= \frac{\log \alpha_1 - \log \alpha_3}{g_3}. \end{aligned} \tag{3.24}$$

Taking exponentials on both sides gives the steady-state concentrations. This example will be revisited in Problem 4.8.15, which illustrates how further insight can be drawn directly from these explicit descriptions.

Exercise 3.5.1 Consider the irreversible three-step reaction chain $\rightarrow S_1 \rightarrow S_2 \rightarrow$. Formulate an S-system description of the system, presuming a constant input rate α_0 and GMA reaction rates $\alpha_1[S_1]^{g_1}$ and $\alpha_2[S_2]^{g_2}$. Derive explicit formulas for the steady state concentrations of s_1 and s_2. □

3.6 Suggestions for Further Reading

- **Enzyme Kinetics:** A concise introduction to enzyme kinetics can be found in *Enzyme Kinetics* (Cornish-Bowden and Wharton, 1988). A more complete description is provided in *Fundamentals of Enzyme Kinetics* (Cornish-Bowden, 1979). More recent treatments are *Enzyme Kinetics and Mechanism* (Cook and Cleland, 2007), and *Enzyme Kinetics for Systems Biology* (Sauro, 2010).
- **Compartmental Modelling:** An extensive treatment of compartmental modelling is provided in *Compartmental Analysis in Biology and Medicine* (Jacquez, 1985).
- **S-system Modelling:** S-system modelling is introduced by Michael Savageau in his book *Biochemical Systems Analysis: a study of function and design in molecular biology* (Savageau, 1976). An updated treatment is given in *Computational Analysis of Biochemical Systems: a practical guide for biochemists and molecular biologists* (Voit, 2000).

3.7 Problem Set

3.7.1 Michaelis-Menten kinetics: estimation of parameters.
a) How would you estimate the Michaelis-Menten parameters $V_{\max}$ and K_M from a *Lineweaver-Burk plot*: a linear plot of $1/v$ against $1/s$ (where v is the reaction rate, or velocity).
b) An alternative formulation, suggested by Hanes and Woolf is to rearrange the kinetic description to yield a linear equation for $\frac{s}{V}$ as a function of s. Derive this formula.

3.7.2 Michaelis-Menten kinetics: separation of time-scales. The separation of time-scales that was used to derive the Michaelis-Menten rate law (3.5) from reaction scheme (3.2) depends on the substrate being much more abundant than the catalysing enzyme. This separation of timescales can be formalized as follows.
a) Rescale the variables in system (3.3) by defining $C = c/e_T$ and $S = s/s(0)$, where e_T is the total enzyme concentration and $s(0)$ is the initial concentration of substrate. These new variables are dimensionless ratios. Show that these scaled concentrations S and C satisfy

$$\begin{aligned} \frac{s(0)}{e_T}\frac{d}{dt}S(t) &= -k_1 S(t)s(0)(1-C(t)) + k_{-1}C(t) \\ \frac{d}{dt}C(t) &= k_1 S(t)s(0)(1-C(t)) - (k_{-1}+k_2)C(t). \end{aligned}$$

b) Explain why this set of equations exhibits a difference in time-scales when $\frac{s(0)}{e_T}$ is large. Hint: the terms describing the dynamics on right-hand-side of these equations are of roughly the same size (they are virtually the same, except for the sign). How then, will the size of $\frac{dS}{dt}$ compare to the size of $\frac{dC}{dt}$?

3.7.3 Reversible Michaelis-Menten kinetics.
a) Derive the reversible Michaelis-Menten rate law (equation (3.9)) as follows. Apply a quasi-steady state assumption to the complex C in reaction scheme (3.8) to arrive at a description of its concentration:

$$c^{qss} = \frac{k_1 e_T s + k_{-2} e_T p}{k_1 s + k_{-2} p + k_{-1} + k_2}.$$

Next, confirm that the reaction rate is

$$v = \frac{d}{dt}p(t) = \frac{k_1 k_2 e_T s - k_{-1} k_{-2} e_T p}{k_1 s + k_{-2} p + k_{-1} + k_2}.$$

b) Express the parameters in equation (3.9) (i.e. V_f, V_r, K_S, K_P) in terms of the rate constants k_1, k_2, k_{-1} and k_{-2}.
c) Confirm that when k_{-2} is zero, the irreversible Michaelis-Menten rate law is recovered.

3.7.4 Product inhibition. Many enzymatic reactions that are irreversible are nevertheless subject to *product inhibition*, meaning that the product readily re-binds the free enzyme. To describe product inhibition, consider the scheme:

$$S + E \underset{k_{-1}}{\overset{k_1}{\rightleftharpoons}} C_1 \xrightarrow{k_r} C_2 \underset{k_{-2}}{\overset{k_2}{\rightleftharpoons}} P + E,$$

which is equivalent to scheme (3.1), except the conversion step is irreversible. From this reaction scheme, derive the rate law

$$\frac{d}{dt}p(t) = v = \frac{V_m s}{s + K_m(1 + \frac{p}{K_P})},$$

3.7.5 Michaelis-Menten kinetics: first-order approximation. Consider the reaction chain

$$\xrightarrow{v_0} S_1 \xrightarrow{v_1} S_2 \xrightarrow{v_2} S_3 \xrightarrow{v_3}$$

in which the v_i are labels for the reaction rates (not mass-action constants). Take the rate v_0 as fixed and presume the other reactions follow Michaelis-Menten kinetics, with

$$v_i = \frac{V^i_{\max} s_i}{K_{Mi} + s_i},$$

where $s_i = [S_i]$. Take parameter values (in mM/min) $v_0 = 2$, $V^1_{\max} = 9$, $V^2_{\max} = 12$, $V^3_{\max} = 15$; (in mM) $K_{M1} = 1$, $K_{M2} = 0.4$, $K_{M3} = 3$.
a) Simulate the system from initial conditions (in mM) $(s_1, s_2, s_3) = (0.3, 0.2, 0.1)$. Repeat with initial condition $(s_1, s_2, s_3) = (6, 4, 4)$.
b) Generate an approximate model in which the rates of reactions 1, 2, and 3 follow first-order mass action kinetics (i.e. $v_i = k_i s_i$, for $i = 1, 2, 3$). Choose values for the rate constants k_i that give a good approximation to the original nonlinear model. Explain your reasoning. (Hint: Exercise 3.1.2(b) provides one viable approach.)
c) Simulate your simpler (mass-action based) model from the sets of initial conditions in part (a). Comment on the fit. If the approximation is better in one case than the other, explain why.

3.7.6 Michaelis-Menten kinetics: double-displacement reactions. Recall the double-displacement (ping-pong) mechanism for an irreversible enzyme-catalysed two-substrate reaction as described in Section 3.1.2. Suppose the reaction scheme is

$$A + E \underset{k_{-1}}{\overset{k_1}{\rightleftharpoons}} C_1 \xrightarrow{k_2} P + E^*$$
$$B + E^* \underset{k_{-3}}{\overset{k_3}{\rightleftharpoons}} C_2 \xrightarrow{k_4} Q + E$$

Derive a rate law as in equation (3.12) by using the conservation $e_T = [E] + [C_1] + [E^*] + [C_2]$ and applying a quasi-steady state assumption to the substrate-enzyme complexes (C_1 and C_2) and to the modified enzyme E^*. You should find that the constant term K_{AB} in the denominator is zero.

3.7.7 Specificity constants. Some enzymes catalyse multiple reactions. When distinct substrates compete for an enzyme's catalytic site, they act as competitive inhibitors of one another. In this context, we can define the *specificity constant* for each substrate as the ratio of the enzyme's corresponding catalytic constant, k_{cat} (k_2 in scheme (3.2)), to the substrate's Michaelis constant, K_M:

$$\text{specificity constant: } \; k_s = \frac{k_{\text{cat}}}{K_M}.$$

Suppose two species, S and S' are both substrates for an enzyme E. Verify that the ratio of the reaction rates for S and S' is the product of the ratio of their concentrations and the ratio of their specificity constants:

$$\frac{\text{rate of reaction of } S}{\text{rate of reaction of } S'} = \frac{[S]}{[S']} \cdot \frac{k_s}{k_{s'}}$$

Hint: There is no need to construct a reaction scheme. Take the rate of reaction of S to be $\frac{e_T k_{\text{cat}}[S]}{K_M(1+[S']/K'_M)+[S]}$, and likewise for S'. (That is, the Michaelis constant for S' is equal to its inhibition constant with respect to S, and vice-versa).

3.7.8 Allosteric activation. Consider an allosteric *activation* scheme in which an allosteric activator must be bound before an enzyme can bind substrate. This is called *compulsory activation.* The reaction scheme resembles a two-substrate reaction, but the enzyme-activator complex stays intact after the product dissociates:

$$R + E \quad \underset{k_{-1}}{\overset{k_1}{\rightleftharpoons}} \quad ER$$
$$ER + S \quad \underset{k_{-2}}{\overset{k_2}{\rightleftharpoons}} \quad ERS \xrightarrow{k_3} P + ER,$$

where R is the allosteric activator (regulator).

a) Apply a quasi-steady-state assumption to the two complexes ER and ERS (and use enzyme conservation) to verify that the rate law takes the form

$$v = \frac{srk_3e_T}{r\frac{k_{-2}+k_3}{k_2} + \frac{k_{-1}(k_{-2}+k_3)}{k_1k_2} + sr} = \frac{V_m sr}{K_1 r + K_2 + rs}$$

where r is the regulator concentration and s is the substrate concentration.
b) Next, consider the case in which catalysis can only occur after n regulator molecules have bound. Assuming the the binding involves strong cooperativity, we can approximate the regulator-binding events by:

$$nR + E \quad \underset{k_{-1}}{\overset{k_1}{\rightleftharpoons}} \quad ER_n$$

Verify that in this case the rate law takes the form

$$v = \frac{sr^nk_3e_T}{r^n\frac{k_{-2}+k_3}{k_2} + \frac{k_{-1}(k_{-2}+k_3)}{k_1k_2} + sr^n} = \frac{V_m sr^n}{K_1 r^n + K_2 + r^n s}$$

c) Confirm that when regulator and substrate are at very low concentration, the the rate law in part (b) can be approximated as

$$v = \frac{V_m}{K_2} sr^n.$$

3.7.9 Non-cooperative multi-site binding. An enzyme with multiple binding sites that are independent (no cooperativity) cannot exhibit sigmoidal binding curves, even when the binding sites have distinct affinities. Consider a protein with two ligand binding sites of different affinities. Show that in this case the fractional saturation is simply the sum of two hyperbolic relations:

$$Y = \frac{[X]/K_1}{2(1 + [X]/K_1)} + \frac{[X]/K_2}{2(1 + [X]/K_2)}$$

where K_1 and K_2 are the dissociation constants for the two sites. Plot this relation for various values of K_1 and K_2 to confirm that it describes a hyperbolic binding curve.

3.7.10 Negative cooperativity. The discussion of cooperative binding in Section 3.3 focused on *positive cooperativity*, in which the substrate binding affinity increases as substrates bind. Some proteins, such as the enzyme glyceraldehyde-3-phosphate dehydrogenase, exhibit *negative cooperativity*—substrate affinity drops as substrates bind.
a) Consider the Adair equation for two sites in Exercise 3.3.1. Plot the curve for a negative cooperative case (e.g. for $K_2 > K_1$.) Is the curve sigmoidal?
b) An extreme case of negative cooperativity is known as *half-of-the-sites-reactivity*, in which the affinity drops to zero once half of the binding sites are occupied. Referring again to the Adair equation for two sites, what is the form of the binding curve in this extreme case?

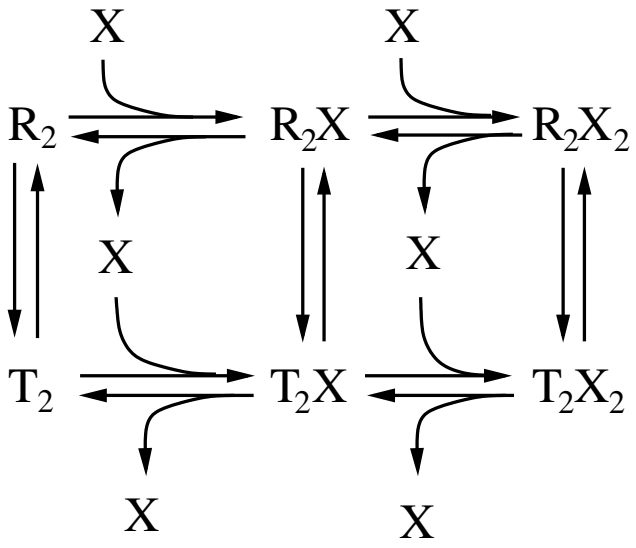

Figure 3.15: Binding scheme for concerted model of cooperativity (Problem 3.7.11).

3.7.11 The concerted model of cooperativity. In 1965 Jacques Monod, Jeffries Wyman and Jean-Pierre Changeux proposed a mechanistic model of cooperativity (Monod *et al.*, 1965). Their model addresses a multimeric protein composed of identical subunits, each with one ligand binding site. They supposed that each subunit could transition between two conformations: a tensed state T, and a relaxed state R. For each protein molecule, all of the subunits are presumed to have the same conformation at any given time: transitions between the relaxed and tense states are *concerted*.

In the absence of ligand, the tensed state is more stable than the relaxed state. The relaxed state, however, has a higher affinity for ligand. Thus, at a sufficiently high ligand concentration, ligand binding causes the protein to adopt the relaxed state. This increases the protein's affinity for ligand, triggering a positive feedback, and resulting in a sigmoidal binding curve.

This mechanism is called the *MWC model*, or the *concerted model*. The ligand-binding scheme for a dimer is shown in Figure 3.15, where R_2 is the dimer of two relaxed monomers and T_2 is the dimer of two tensed monomers.

a) Let K be the equilibrium constant for the $R_2 \leftrightarrow T_2$ conversion (i.e. $K = [T_2]/[R_2]$ at steady state). Suppose that the dissociation constant for ligand binding to R_2 is K_R, while the dissociation constant for ligand binding to T_2 is K_T. (The dissociation constants for the first and second binding events are the same, but the association/dissociation rates will depend on stoichiometric factors that reflect the number of sites.)

Confirm that in steady state, the concentrations satisfy

$$[R_2] = \frac{T_2}{K} \qquad [R_2X_1] = \frac{2[X][R_2]}{K_R} \qquad [R_2X_2] = \frac{[X][R_2X_1]}{2K_R}$$
$$[T_2X_1] = \frac{2[X][T_2]}{K_T} \qquad [T_2X_2] = \frac{[X][T_2X_1]}{2K_T}.$$

(The stoichiometric pre-factors reflect the availability of binding sites.) Use these equilibrium

conditions to verify that in steady state the fractional saturation is given by

$$Y = \frac{K\frac{[X]}{K_T}\left(1+\frac{[X]}{K_T}\right) + \frac{[X]}{K_R}\left(1+\frac{[X]}{K_R}\right)}{K\left(1+\frac{[X]}{K_T}\right)^2 + \left(1+\frac{[X]}{K_R}\right)^2}, \tag{3.25}$$

Plot the corresponding binding curves for $K_T = 1000$, $K_R = 1$, and $K = 500$, 1000, and 2000. Verify that although this is not a Hill function, the curves are nevertheless sigmoidal.
b) Consider the special case of the concerted mechanism in which $K = 0$. Interpret the resulting binding mechanism and use formula (3.25) to verify that the resulting binding curve is hyperbolic. Repeat for the case when $K_R = K_T$.
c) Verify that when the concerted model is applied to a tetramer (such as hemoglobin), the resulting fractional saturation is

$$Y = \frac{K\frac{[X]}{K_T}\left(1+\frac{[X]}{K_T}\right)^3 + \frac{[X]}{K_R}\left(1+\frac{[X]}{K_R}\right)^3}{K\left(1+\frac{[X]}{K_T}\right)^4 + \left(1+\frac{[X]}{K_R}\right)^4}.$$

3.7.12 Compartmental modelling: diffusion. Consider a system composed of three compartments: Compartment 1, the nucleus, with volume V_1; Compartment 2, the cytosol, with volume V_2; and Compartment 3, the surrounding extracellular space, with volume V_3.
a) Suppose that a molecular species S can diffuse across the nuclear membrane and across the cellular membrane. Confirm that the species concentrations s_i in compartment i satisfy

$$\begin{aligned}
\frac{d}{dt}s_1(t) &= \frac{D_1}{V_1}(s_2(t) - s_1(t)) \\
\frac{d}{dt}s_2(t) &= \frac{D_1}{V_2}(s_1(t) - s_2(t)) + \frac{D_2}{V_2}(s_3(t) - s_2(t)) \\
\frac{d}{dt}s_3(t) &= \frac{D_2}{V_3}(s_2(t) - s_3(t)),
\end{aligned}$$

where D_1 and D_2 characterize diffusion across the nuclear and cell membrane, respectively.
b) Suppose that the initial concentrations are s_1^0, s_2^0, and s_3^0. Verify that at steady state:

$$s_1^{ss} = s_2^{ss} = s_3^{ss} = \frac{s_1^0 \cdot V_1 + s_2^0 \cdot V_2 + s_3^0 \cdot V_3}{V_1 + V_2 + V_3}.$$

c) Suppose now that the concentration of S in the extracellular space is buffered, so that $s_3 = \bar{s}_3$ (constant). Verify that in this case the steady state is given by

$$s_1^{ss} = s_2^{ss} = \bar{s}_3$$

d) Continuing with the buffered concentration assumption in part (c), suppose that species S is produced in the nucleus at rate k, i.e.

$$\frac{d}{dt}s_1(t) = \frac{D_1}{V_1}(s_2(t) - s_1(t)) + k$$

Determine the steady state concentrations of s_1^{ss} and s_2^{ss} in this case. How does the difference $s_1^{ss} - s_2^{ss}$ depend on the model parameters? Interpret your results.

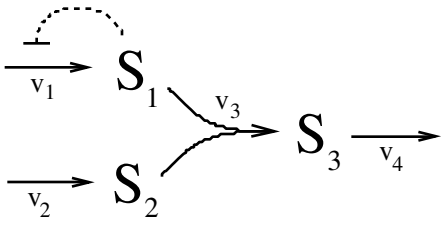

Figure 3.16: Reaction network for Problem 3.7.13.

3.7.13 *S-system modelling. Consider the reaction network in Figure 3.16. Formulate an S-system model of the network, using reaction rates $v_1 = \alpha_1[S_1]^{g_1}$, $v_2 = \alpha_2$, $v_3 = \alpha_3[S_1]^{g_2}[S_2]^{g_3}$, $v_4 = \alpha_4[S_3]^{g_4}$. Derive explicit formulas for the steady state concentrations in terms of the model parameters.